Synthesis of Novel Diselenide-Linked Porphyrin Dimers under Phase-Transfer Catalysis Condition and Their Interactions with DNA

by **Zhi Xue**[a]), **Daniel Wei-Jing Kwong**[b]), **Ling-Wei Xue**[c]), **Qing Liu**[a]), **An-Xin Hou***[a]), and **Wai-Kwok Wong***[a])[b])

[a]) Department of Chemistry, Wuhan University, Wuhan 430072, P. R. China (phone: +86 27 68752323; fax: +86 27 68754067; e-mail: houanxin@yahoo.com)
[b]) Department of Chemistry, Hong Kong Baptist University, Kowloon Tong, Hong Kong SAR, P. R. China (phone: +852 34117011; fax: +852 34117348; e-mail: wkwong@hkbu.edu.hk)
[c]) College of Chemistry and Chemical Engineering, Pingdingshan University, Pingdingshan 467002, P. R. China

Novel diselenide-linked porphyrin dimers were synthesized under phase-transfer catalysis conditions. The targeted compounds were characterized by ^{1}H-NMR, high-resolution mass spectrometry, UV/VIS and fluorescence spectroscopies, redox-potential measurements, and elemental analysis. The interaction of the title compounds with DNA was studied using UV/VIS, fluorescence, and circular dichroism (CD) spectroscopies. The relative rates of singlet-oxygen production from the diselenide-linked porphyrin dimers upon photoirradiation were also measured.

Introduction. – Diselenide compounds such as dialkyl and diaryl diselenides have aroused great interest over the past decades due to their diverse biological properties, ranging from antioxidant [1], glutathione peroxidase (GSHPx)-like [2], anti-inflammatory, and antinociceptive activities [3] to chemopreventive properties towards colon carcinogenesis [4] as well as antitumor properties [5] but with low long-term systemic toxicity [6]. However, the biological effects of Se-containing compounds on cells depend strongly on dosage as well as the specific chemical form used [7]. For instance, at supranutritional dose, Se compounds exhibit chemopreventive action towards many types of cancer [8]. But at higher concentrations, DNA-strand breaks occur, leading to cytotoxic or possibly carcinogenic effects [9]. To avoid the undesirable effects due to an overdosing of normal cells, selective uptake/retention of the Se compounds by the targeted tumor cells is of crucial importance.

Porphyrins, which bind to DNA and exhibit antitumor and antimicrobial activities upon photoirradiation [10][11], have been shown to localize selectively in tumor cells and were used as photodynamic therapeutic (PDT) agents due to their ability to produce singlet oxygen, which can cleave DNA and damage the tumor cells [12]. Even though the mechanism of selective uptake/retention of porphyrins by tumor cells is not completely known [13], attempts have been made to design highly selective tumor-targeting drugs by linking a potent chemotherapeutic moiety, such as cisplatin and taxol, to porphyrin to enhance their antitumor efficacies [14][15]. Furthermore, selective targeting of specific cell types, such as hepatocytes, has been achieved in a galactosylated porphyrin where the β-D-galactose is recognized and then internalized

by the asialoglycoprotein receptor (ASGR) present only on hepatocytes and several hepatoma cell lines at high density [16].

We are interested in investigating the antitumor properties of diselenides conjugated with porphyrins. In this work, we report a convenient method for the preparation of such diselenide-linked porphyrin conjugates in which phase-transfer catalyst (PTC) played an important role. The compounds synthesized were characterized using high-resolution mass spectrometry, ^{1}H-NMR, UV/VIS, and fluorescence spectroscopies, physiologically relevant redox-potential measurements, and elemental analyses. In addition, the interaction of the diselenide-linked porphyrin dimers with herring-sperm DNA (HS DNA) was studied using UV/VIS absorption, fluorescence, and circular dichroism (CD) spectroscopies. The relative rates of singlet-oxygen production from these diselenide-linked porphyrin dimers upon photoirradiation were also measured.

Results and Discussion. – *Synthesis and Characterization of Diselenide-Linked Porphyrin Dimers.* The diselenide-linked porphyrin dimers were prepared for the first time using PTC. The total synthetic route of the title compounds is given in the *Scheme.* Briefly, Na_2Se_2 (**1**) was prepared by a modification of the procedure due to *Klayman* and *Griffin* [17]. Selenium powder was first reduced in H_2O by $NaBH_4$ to **1**. Benzyl(triethyl)ammonium chloride (TEBA), used as the PTC, was added into the aqueous solution of Na_2Se_2. The resulting dark-red solution was set aside for use in a subsequent step. Monohydroxy-substituted porphyrin **2** was synthesized from PhCHO, 1*H*-pyrrole, and 4-hydroxybenzaldehyde. Using a modified literature procedure, bromoalkyl-substituted porphyrins **3** were prepared by an addition of dibromoalkane to **2** under moisture- and O_2-free conditions [18]. Lastly, the aqueous solution of **1** containing the TEBA previously set aside was allowed to react with **3** under PTC condition to afford the final products, diselenide-linked porphyrin dimers **4**.

In this work, three key modifications were made to the literature procedures to accomplish the synthesis of the title compounds **4**. *i*) In the classical method for preparing Na_2Se_2 (**1**), there was always considerable amount of Se powders remaining unreacted [17]. As elemental Se is insoluble in H_2O, addition of a PTC facilitates its solubilization and allows the reaction to proceed smoothly at room temperature to afford **1**. *ii*) According to the literature synthetic procedure for **3** [18], dibromoalkane was added to a suspension of **2** and anhydrous K_2CO_3 in dry DMF. The resulting mixture was then stirred at 60° to afford **3**. But, in this work, *Schlenk* technique was applied to achieve a moisture- and O_2-free condition in this synthesis, resulting in a yield of up to 95%. *iii*) The synthesis of **4** was carried out under PTC condition. Porphyrins **3** were not soluble in H_2O, but **1** was in an aqueous solution. The use of PTC such as TEBA was, therefore, necessary to bring about the reaction between **1** and **3**, resulting in the successful synthesis of the diselenide-linked porphyrin dimers.

The characterization of the title compounds **4a**–**4c** was performed by high-resolution mass spectrometry (HR-MS). The HR-MS data are presented in *Fig. 1*, showing the molecular-ion peaks of these compounds, where their m/z values compared favorably with the calculated ones (*i.e.*, $\Delta_m < 5$ ppm). Further characterization of **4** by ^{1}H- and ^{77}Se-NMR, UV/VIS absorption, and fluorescence spectroscopies was performed. The ^{77}Se-NMR of one diselenide-linked porphyrin dimer, **4a**, is given in

Scheme. *Total-Synthetic Route for Diselenide-Linked Porphyrin Dimers*

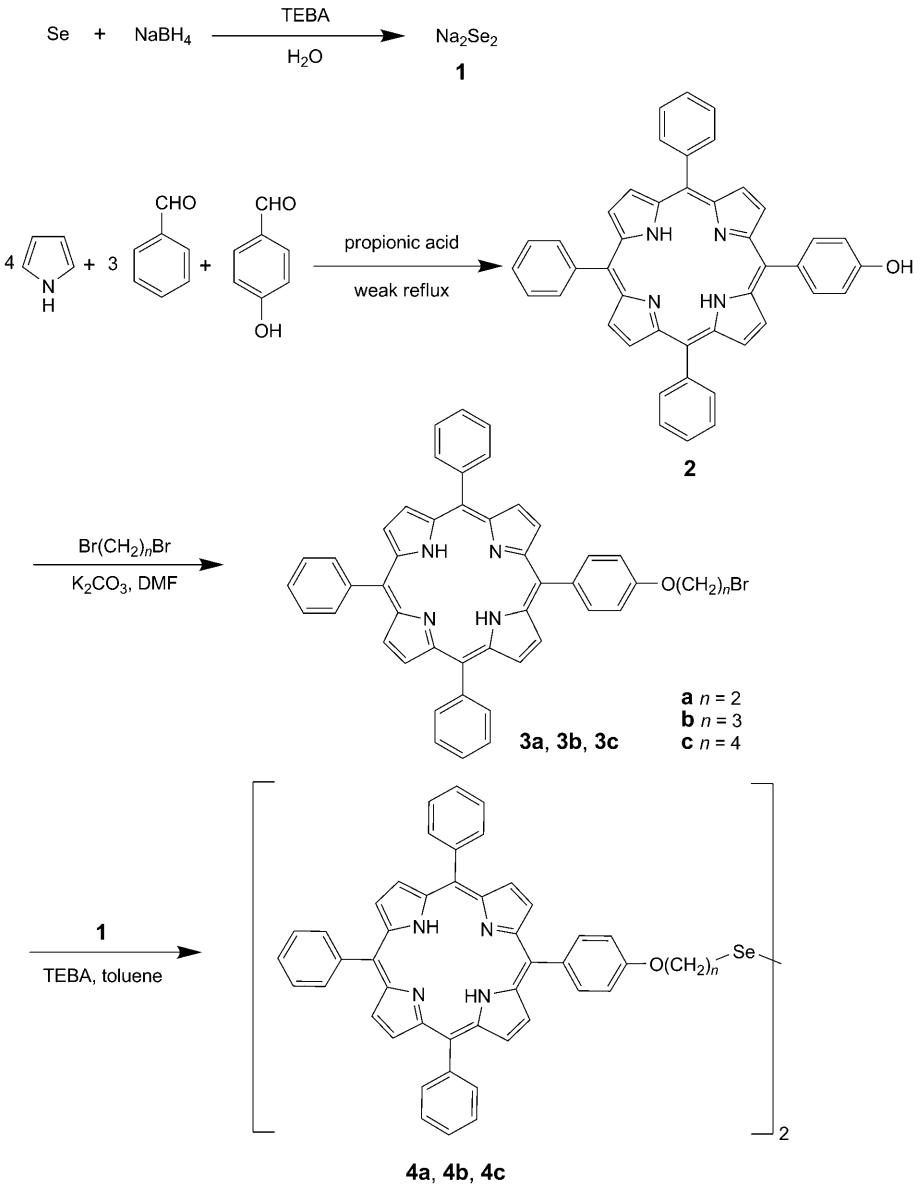

Fig. 2, *a*, where the major *singlet* observed at 20.888 ppm was due to **4a**, and the minor *singlet* observed at 32.669 ppm was due to its monomer, porphyrin-selenol (TPP-$(CH_2)_2$-SeH). The presence of the monomeric porphyrin-selenol in the sample was confirmed by MALDI-TOF-MS (observed m/z 739.150, $[TPP\text{-}(CH_2)_2\text{-}SeH + H]^+$; calc. 739.197). Due to the symmetry of the compound, no Se,Se coupling, which gives direct

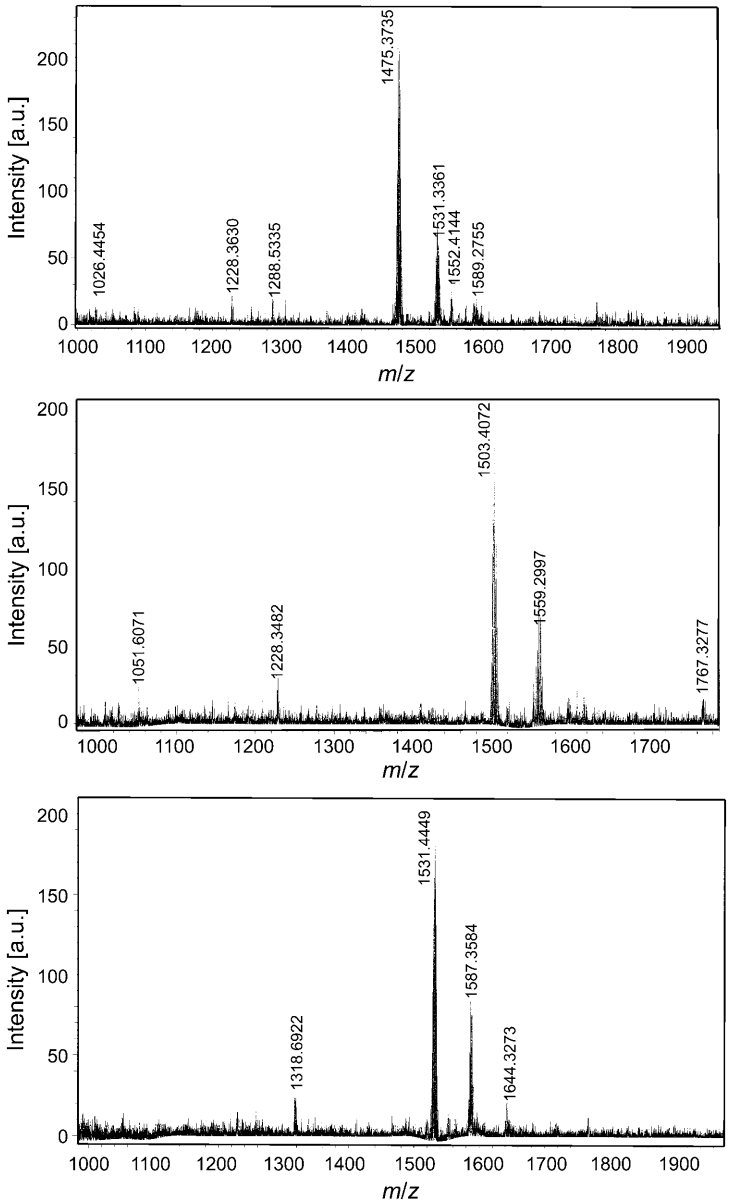

Fig. 1. *HR-MS of* **4a**–**4c** (from top to bottom). For **4a**: *m/z* 1475.3735 ($[M+1]^+$; calc. 1475.3639, $\Delta_m = -0.9489$ ppm). For **4b**: *m/z* 1503.4072 ($[M+1]^+$; calc. 1503.3952, $\Delta_m = 0.5986$ ppm). For **4c**: *m/z* 1531.4449 ($[M+1]^+$; calc. 1531.4265, $\Delta_m = 4.7014$ ppm).

evidence of the presence of Se–Se bond, can be observed. But, the presence of two Se-atoms in these compounds was evidenced by their elemental analysis and the Se-isotope profile of the MALDI-TOF mass spectra of these compounds (see *Fig. 2,b*).

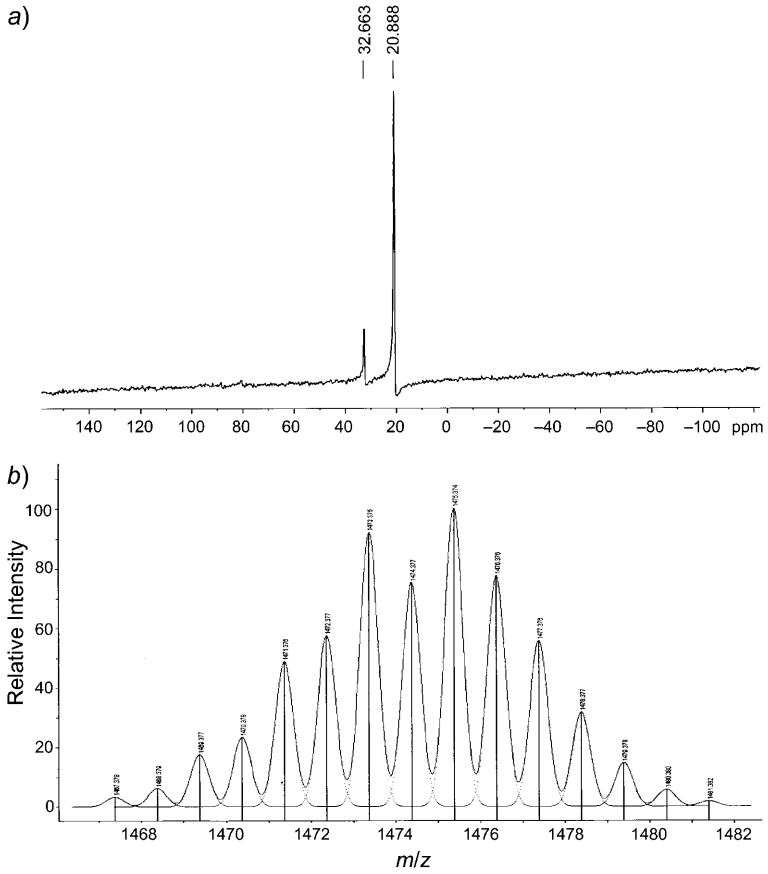

Fig. 2. a) *^{77}Se-NMR Spectrum of the diselenide-linked porphyrin* **4a** *in $CDCl_3$ with Me_2Se as the external reference.* The major *singlet* observed at δ 20.888 was due to **4a**, and the minor *singlet* at δ 32.669 was due to its monomer, porphyrin-selenol (TPP-$(CH_2)_2$-SeH). b) *Selenium isotope profile of MALDI-TOF MS of* **4a**. The solid vertical lines represent the expected (calculated) isotope mass profile of a compound containing two Se-atoms, which matched closely with the peak profile observed for **4a**.

Thus, redox-potential measurement to probe the redox reaction of the Se–Se bond of the diselenide-linked porphyrin dimers **4** by cyclic voltammetry was also conducted.

Redox-Potential Characterization. To further characterize the compounds **4**, the redox properties of the three diselenide-linked porphyrin dimers were studied by cyclic voltammetry. In this study, water-soluble multi-walled carbon nanotubes (MWCNT)-modified gold (Au) electrode was chosen over other common electrodes (such as Pt and glassy C electrodes), as it gave a better signal, presumably due to its larger surface area and enhanced reactivity [19]. *Fig. 3* shows the cyclic voltammograms of **4** and 5,10,15,20-tetraphenylporphyrin (H_2TPP), which was included as a reference compound for the porphyrin moiety in **4**, on the modified Au electrode. For H_2TPP, no

distinct redox peak was observed in the potential range from 0 to −1.0 V in 0.1M phosphate buffer, pH 7.4 (*Fig. 3*,*a*). However, distinct reduction peaks were observed for the three diselenide-linked porphyrin dimers, **4a**–**4c**, adsorbed on the MWCNT-modified Au electrode. The voltammograms of these diselenide-linked porphyrins differ from each other only slightly in the number and potential values of their reduction peaks (*Fig. 3*,*b*–*d*). More importantly, all of them exhibit an almost identical oxidation peak at around −0.70 V, suggesting the same origin of the reduction peaks for these compounds, *i.e.*, the reduction of the Se–Se bond. The reduction peak potential values observed (*e.g.*, −0.79 V in **4b** and −0.80 V in **4c**) were comparable to the range of −0.5 to −0.7 V observed for other diselenides [20]. The slight difference in the reduction peaks for the three Se samples might arise from the different chemical environments of the Se–Se bond in the three porphyrin dimers.

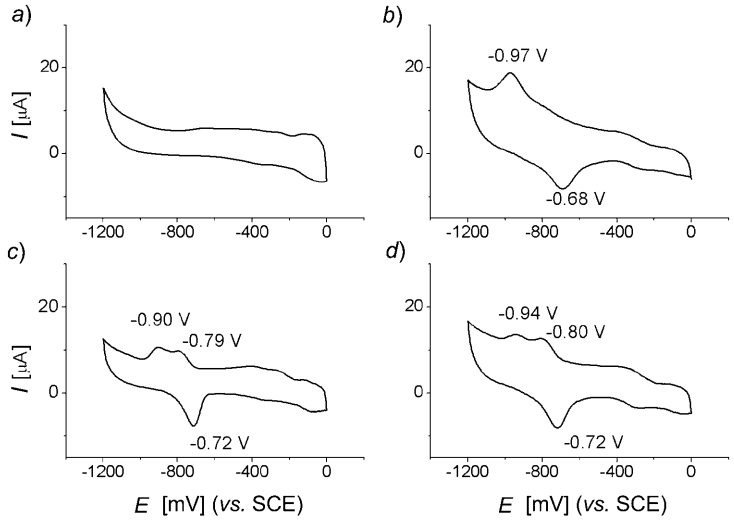

Fig. 3. *Cyclic voltammograms of H_2TPP* (*a*) *and the diselenide-linked porphyrin dimers* **4a**–**4c** (*b*–*d*, resp.) *adsorbed on MWCNT-modified gold electrode in 0.1M phosphate buffer solution* (pH 7.4) *measured at a scan rate of 100 mV/s*

UV/VIS- and Fluorescence-Spectroscopic Studies of Diselenide-Linked Porphyrin Dimer–DNA Interactions. Most studies on porphyrin–DNA interactions were performed using monoporphyrins; only few reports have appeared on porphyrin dimers [21][22]. Here, we report the results of our spectrophotometric titration study of the interactions between DNA and the diselenide-linked porphyrin dimers **4**. *Fig. 4* (left) shows the spectral changes of the *Soret* band of the porphyrins (**4a**–**4c**) at near 430 nm upon addition of HS DNA. Moderate red shift of the *Soret* band ($\Delta\lambda = 4$–9 nm), together with a significant hypochromic effect (55–74%), were observed for the porphyrin dimer, *e.g.*, a red shift up to 9 nm and a hypochromicity of 55% were observed in **4b**. The detailed spectral changes are collected in the *Table.*

In most porphyrin–DNA interactions studied, three distinct binding modes, namely, intercalative binding, external groove binding, and outside binding with self-stacking along the DNA helix have been documented [22]. Among these three binding

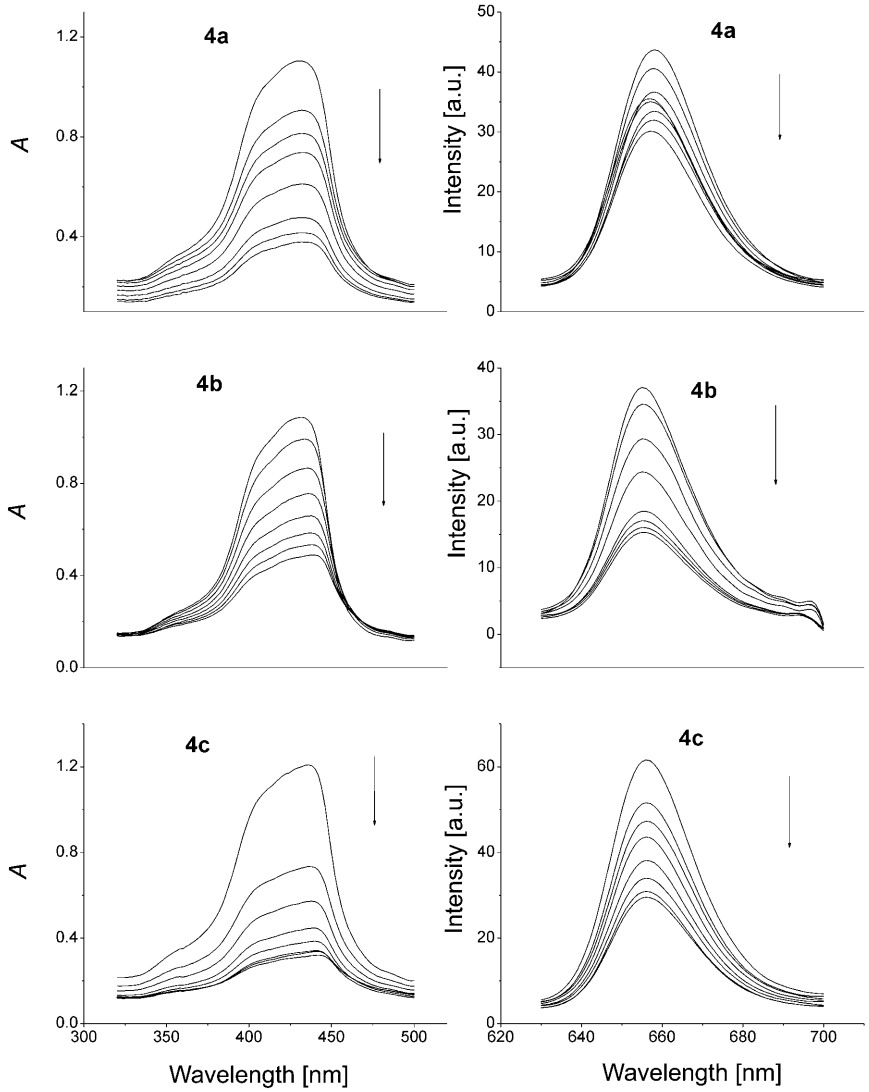

Fig. 4. Left: *UV/VIS Absorption spectra of the diselenide-linked porphyrin dimers* **4a**–**4c** (10 μM) *in the presence of increasing concentrations of HS DNA, expressed as ratio of* c_{DNA}/c_{por} *= 0, 0.1, 0.2, 0.4, 0.8, 1.2, 1.6, 3.2, resp., at pH 7.4.* Right: *Fluorescence spectra of* **4a**–**4c** (10 μM) *with increasing concentrations of HS DNA, corresponding to the same* c_{DNA}/c_{por} *ratios of those in the UV/VIS titration spectra.*

modes, intercalative binding is characterized by a substantial red shift (>10 nm) and a significant hypochromicity (up to 40%) of the *Soret* band. External groove binding is characterized by a minor-to-insignificant spectral shift and an occasional hyperchromicity. As for those prophyrins that interact with DNA *via* the outside binding with self-stacking mode, similar spectral characteristics as in the intercalative binding mode

Table. *UV/VIS Absorption- and Fluorescence-Spectral Changes of the Diselenide-Linked Porphyrin Dimers* **4a**–**4c** *upon Titration with HS DNA*[a])

Porphyrin dimer	UV/VIS Spectral data of the *Soret* band		Fluorescence
	Red shift [nm]	Hypochromicity [%]	Intensity decrease [%]
4a	4	65.7	26.9
4b	9	55.0	58.7
4c	6	73.5	52.5

[a]) The sample mixtures contained 10 μM of the porphyrin dimers, **4a**–**4c**, and HS DNA in different molar ratios, *i.e.*, $c_{DNA}/c_{porphyrin} = 0$ and 10. All experiments were performed at room temperature in 0.05M *Tris*·HCl buffer, pH 7.4, containing 0.1M NaCl.

are seen [22]. According to this criterion, these diselenide-linked porphyrin dimers, **4a**–**4c**, appeared to bind to DNA *via* outside binding with self-stacking along the DNA helix (*vide infra*).

For those porphyrin–DNA interactions showing significant red shift and hypochromicity, an apparent binding constant (K_{app}) can be calculated according to *Eqn. 1:*

$$\frac{[DNA]_{total}}{(|\varepsilon_{app} - \varepsilon_f|)} = \left\{\frac{1}{(|\varepsilon_b - \varepsilon_f|)}\right\}[DNA]_{total} + \frac{1}{\{K_{app}(|\varepsilon_b - \varepsilon_f|)\}} \quad (1)$$

where ε_{app}, ε_f, and ε_b correspond to $A_{obs}/[porphyrin]$, the extinction coefficient for the free porphyrin, and the extinction coefficient for the porphyrin in the fully bound form, respectively. From a plot of $[DNA]_{total}/(|\varepsilon_{app} - \varepsilon_f|)$ *vs.* $[DNA]_{total}$, shown in *Fig. 5*, K_{app} is obtained by the ratio of the slope to the intercept [23]. The K_{app} values of **4a**–**4c** were determined to be 2.57×10^5, 2.09×10^5, and 1.24×10^6 M^{-1}, respectively. These spectral changes and K_{app} values obtained for the diselenide-linked porphyrin dimers are comparable to those observed in another porphyrin dimer, *i.e.*, 4,4′-dicarboxy-2,2′-bipyridine-5-(4-aminophenyl)-10,15,20-tripyridin-4-ylporphyrin ($\Delta\lambda = 9$ nm, hypochromicity $H = 37\%$, $K_{app} = 1.2 \times 10^6$ M^{-1}) [24]. These K_{app} values are also comparable to those obtained in most monoporphyrin–DNA interactions, such as in *cis*- and *trans*-

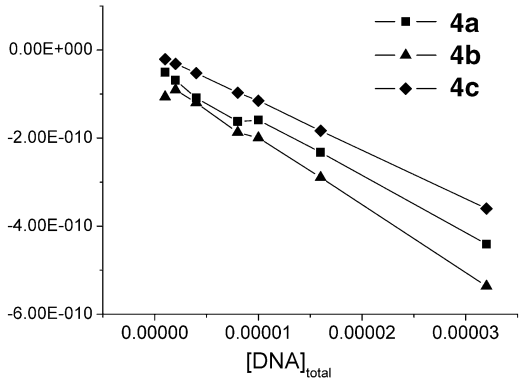

Fig. 5. *Plot of* $[DNA]_{total}/(|\varepsilon_{app} - \varepsilon_f|)$ vs. $[DNA_{total}]$ *for* **4a**–**4c** *in the presence of increasing concentrations of HS DNA*

bis(1-methylpyridinium-4-yl)diphenylporphyrin ($K_{app} = 1.2 \times 10^6$ and 1.4×10^6 M^{-1}, resp.), where intercalative binding modes with DNA were adopted [25].

Fluorescence spectroscopy was also applied to study the interactions of these porphyrin dimers with DNA [26]. The fluorescence emission spectra of **4a**–**4c** ($\lambda_{em,max}$ = 659, 656, and 655 nm, resp.) obtained from titration with increasing concentrations of HS DNA are shown in *Fig. 4* (right). The fluorescence intensities of **4a**–**4c** were quenched to various extents with only minor spectral shifts upon DNA addition. These data are listed also in the *Table*. Such observed fluorescence quenching is consistent with the binding mode suggested by the *Soret*-band titration data, namely, outside binding with self-stacking along the DNA helix. Actually, this binding mode with DNA is expected for all porphyrins with bulky substituents [25]. In this case, the bulky substituent present in **4a**–**4c** is the second porphyrin moiety, which is quite capable of self-stacking.

CD Spectra of Diselenide-Linked Porphyrin–HS DNA Interactions. To further clarify the binding mode, the induced CD spectra of the porphyrins **4** were recorded in the presence of HS DNA (*Fig. 6*). In the case of duplex DNA, a positive-induced CD band in the *Soret* region indicates its groove binding, and a negative induced CD band indicates intercalation [27]. Conservative (or bisignate) CD signal is a signature of self-stacked porphyrins bound externally on the polymer surface [27]. As seen from *Fig. 6*, porphyrins **4a**–**4c** showed the typical conservative CD profiles. For instance, porphyrin **4a**, upon binding to HS DNA, showed a strong positive peak centered at 418 nm and a strong negative peak centered at 440 nm with the intensity of the two peaks being almost identical. All these data were presented in the *Table*. No significant CD signal was observed in DNA alone without the porphyrins or *vice versa* (data not shown). Thus, the bisignate CD feature of **4** suggests an external binding mode with self-stacking, presumably along the helical structure of DNA. This result corroborated with the binding mode inferred from the absorption and fluorescence titration experiments.

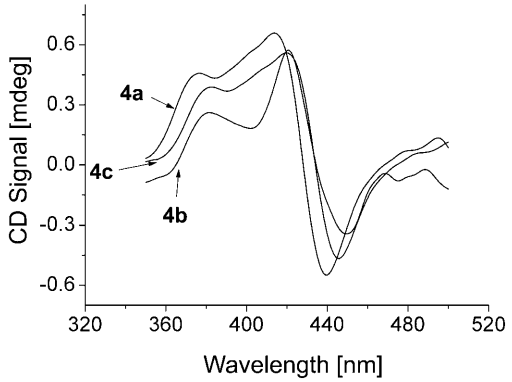

Fig. 6. *Induced CD spectra of* **4a**–**4c** (5 μM) *in the presence of HS DNA* (base-pair concentration 100 μM) *in 0.05*M *Tris·HCl buffer* (pH 7.4), *containing 0.1*M *NaCl*

Singlet-Oxygen Production by Diselenide-Linked Porphyrin Dimers. The relative rates of singlet-oxygen production by the diselenide-linked porphyrin dimers **4a**–**4c** upon photoirradiation were determined using the singlet-oxygen quencher, 1,3-

diphenylisobenzofuran (DPBF), in benzene. The consumption of DPBF (λ_{max} 415 nm) was monitored spectrophotometrically as function of photoirradiation time of **4a**–**4c** with H_2TPP, whose singlet-oxygen yield was reported to be 0.62 in benzene, used as a reference [28]. This result is shown in *Fig. 7*, from which we can see that the rates of singlet-oxygen production from all three diselenide-linked porphyrin dimers were comparable to that of the H_2TPP reference, indicating that the diselenide linkage did not alter the singlet-oxygen quantum yield of the porphyrin moiety significantly.

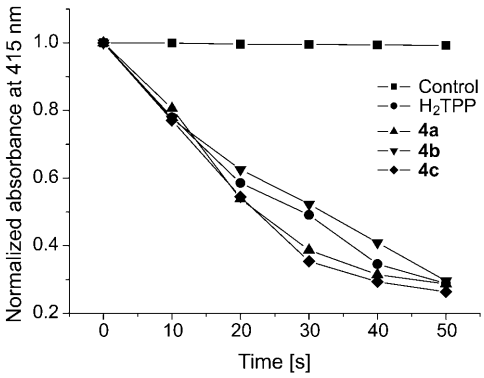

Fig. 7. *Bleaching of 1,3-diphenylisobenzofuran* (DPBF) *by the singlet-oxygen produced from the diselenide-linked porphyrin dimers*, **4a**–**4c**, *and the tetraphenylporphyrin* (H_2TPP) *reference as a function of the photoirradiation time*

Conclusions. – In this work, we reported a convenient synthesis of three diselenide-linked porphyrin dimers. The success of this synthesis rests on the use of a PTC, which facilitated *i*) the reduction of elemental Se to selenide in water and *ii*) the coupling of porphyrin with Na_2Se_2. The binding mode of these porphyrin dimers with DNA was consistent with outside binding with self-stacking along the DNA helix, based on UV/VIS-absorption and fluorescence titration as well as induced CD studies. The singlet-oxygen yields of these compounds were shown to be comparable to that of the H_2TPP. Further studies of the biological activities of these porphyrin dimers are currently underway.

W.-K. W. thanks the *Hong Kong Baptist University* (FRG/05-06/II-03) and *Hong Kong Research Grants Council* (HKBU 2023/04P) for financial support of this work.

Experimental Part

General. Selenium powder, $NaBH_4$, 4-hydroxybenzaldehyde, 1*H*-pyrrole, propanoic acid, 1,2-dibromoethane, 1,3-dibromopropane, 1,4-dibromobutane, DMF, toluene, and benzyl(triethyl)ammonium chloride (TEBA), all of reagent grade, were obtained from *Aldrich Chemical Company*, and were appropriately degassed before use. Solvents were dried by standard procedures, distilled, and deaerated prior to use. UV/VIS Spectra: *OLIS Cary 15* spectrophotometer, λ_{max} in nm (log ε). CD: *JASCO J-810* spectrometer. ^{1}H-NMR Spectra: *JEOL* JNM-EX 270 spectrometer (with TMS as internal standard in $CDCl_3$), δ in ppm, *J* in Hz. ^{77}Se-NMR Spectra: *Bruker* 400-MHz FT-NMR spectrometer *AVANCE III* (^{77}Se = 76.33 MHz) operating in *Fourier*-transform mode at 292.6 K. The sample was run in 5-mm NMR

tube. The ^{77}Se chemical shifts were externally referenced to Me_2Se (60% in $CDCl_3$ at 292.2 K, δ 0.0) by the sample-tube replacement technique. Low-resolution mass spectra (LR-MS): *Finnigan MAT SSQ-710* mass spectrometer, in positive-ion mode. HR-MS: *Bruker Biflex III* matrix-assisted laser desorption/ionization time-of-flight (MALDI-TOF) mass spectrometer, in *m/z*. Fluorescence spectra: *PTI QM-1* spectrofluorometer. Elemental analyses were run on a *Thermo Finnigan Flash EA-1112* series analyzer.

Multi-walled carbon nanotubes (MWCNT; purity >95 wt%, *Timesnano* Co., Chengdu, China) were used as received. Congo red (CR) was purchased from *Shanghai Reagent* Co., Shanghai, China. Cyclic voltammetric (CV) measurements were conducted with an *EG&G* model *283* electrochemical workstation (*Princeton Applied Research*, USA) controlled by a *M270* software. The electrode system consisted of a water-soluble MWCNT film-coated Au electrode, a Pt wire counter electrode, and a KCl-saturated calomel reference electrode (SCE). All potential values in this work were reported against the SCE value.

Synthetic Procedures. Synthesis of H_2TPP. H_2TPP was conveniently prepared according to the procedure described in [18]. It served as a reference compound for the measurements of the redox potentials and the singlet-oxygen production rates of the diselenide-linked porphyrin dimers.

Synthesis of Na_2Se_2 (**1**). Selenium powder (4.5 g, 56 mmol) and TEBA (0.1 g) were added to H_2O (25 ml) in a stoppered three-necked flask with magnetic stirring. $NaBH_4$ (4.5 g, 119 mmol) dissolved in H_2O (25 ml) was added dropwise to the slurry of elemental Se. The flask was chilled in an ice bath to prevent boiling. After all $NaBH_4$ had been added, and the soln. had become colorless, additional Se powder (4.5 g, 56 mmol) was added to the soln., which then turned reddish brown, characteristic of Na_2Se_2. The flask was then stoppered and flushed with Ar.

Synthesis of 5-(4-Hydroxylphenyl)-10,15,20-triphenylporphyrin (**2**). Compound **2** was prepared by a modification of the method described in [18]. A soln. of PhCHO (5.5 ml, 54 mmol) and 4-hydroxybenzaldehyde (3.8 ml, 35 mmol) in propanoic acid (250 ml) was heated to reflux with mechanical stirring. Then, freshly distilled 1*H*-pyrrole (5.0 ml, 72 mmol) in propanoic acid (50 ml) was added dropwise to the soln. After reflux for 1/2 h, the mixture was cooled to r.t. MeOH (300 ml) was then added to the mixture. The resulting soln. was kept in a refrigerator overnight. Filtration gave *ca.* 1.3 g of crude product, which was redissolved in a minimum amount of $CHCl_3$ and chromatographed on a silica-gel column with CH_2Cl_2 as eluent. The second band gave **2** (1.10 g, 5%). FAB-MS (pos.): 631 ($[M+H]^+$).

Synthesis of 5-[4-(2-Bromoethoxy)phenyl]-10,15,20-triphenylporphyrin (**3a**). Compound **3** was prepared according to a modification of the procedure described in [18]. Anh. **2** (0.50 g, 0.8 mmol) and K_2CO_3 (1.0 g) were placed in a *Schlenk* tube, and the mixture was heated to dryness in vacuum to ensure an absolute moisture-free condition. Then, under N_2, anh. DMF (20 ml) and 1,2-dibromoethane (2 ml, 23.1 mmol) were injected into the *Schlenk* tube with a syringe. With magnetic stirring, the mixture was heated at 60°. The progress of the reaction was monitored by TLC. When **2** had been completely converted, DMF in the tube was evaporated in vacuum. The residue was redissolved in $CHCl_3$ and chromatographed (silica-gel column; $CHCl_3$/hexane 5:1). The first band gave **3a** (0.53 g, 90%). ^{1}H-NMR ($CDCl_3$, 270 MHz): 8.80–8.87 (*m*, 8 H pyrrole); 7.26–8.22 (*m*, 19 arom. H); 4.39 (*t*, CH_2O); 3.78 (*t*, CH_2Br); −2.77 (*s*, 2 NH). FAB-MS (pos.): 736 (M^+). Anal. calc. for $C_{46}H_{33}BrN_4O$: C 74.90, H 4.51, N 7.59; found: C 74.82, H 4.60, N 7.52.

Synthesis of 5-[4-(3-Bromopropoxy)phenyl]-10,15,20-triphenylporphyrin (**3b**). Anh. **2** (0.50 g, 0.8 mmol) and K_2CO_3 (1.0 g) were placed in a *Schlenk* tube, and the mixture was heated to dryness in vacuum. Then, under N_2, anh. DMF (20 ml) and 1,3-dibromopropane (2 ml, 19.6 mmol) were injected. As described for **3a**, **3b** (0.54 g, 90%) was obtained. ^{1}H-NMR ($CDCl_3$, 270 MHz): 8.78–8.87 (*m*, 8 H, pyrrole); 7.26–8.22 (*m*, 19 arom. H); 4.25 (*t*, CH_2O); 3.60 (*t*, CH_2Br), 2.51 (*m*, $CH_2CH_2CH_2Br$); −2.78 (*s*, 2 NH). FAB-MS (pos.): 750 (M^+). Anal. calc. for $C_{47}H_{35}BrN_4O$: C 75.10, H 4.69, N 7.45; found: C 75.02, H 4.76, N 7.49.

Synthesis of 5-[4-(4-Bromobutoxy)phenyl]-10,15,20-triphenylporphyrin (**3c**). Anh. **2** (0.50 g, 0.8 mmol) and K_2CO_3 (1.0 g) were placed in a *Schlenk* tube, and the mixture was heated to dryness in vacuum. Then under N_2, anh. DMF (20 ml) and 1,4-dibromobutane (2 ml, 16.7 mmol) were injected. As described for **3a**, **3c** (0.56 g, 92%) was obtained. FAB-MS (pos.): 764 (M^+). ^{1}H-NMR ($CDCl_3$, 270 MHz) 8.87–8.88 (*m*, 8 H, pyrrole); 7.26–8.22 (*m*, 19 arom. H); 4.15 (*t*, CH_2O); 3.55 (*t*, CH_2Br); 2.24 (*m*,

$OCH_2CH_2CH_2CH_2Br$); 2.13 (*m*, $OCH_2CH_2CH_2CH_2Br$); −2.75 (*s*, 2 NH). Anal. calc. for $C_{48}H_{37}BrN_4O$: C 75.29, H 4.87, N 7.32; found: C 75.41, H 4.80, N 7.34.

Synthesis of Diselenide-Linked Porphyrin Dimer **4a** *from* **3a**. To a soln. of **3a** (0.1 g, 0.14 mmol), TEBA (0.01 g) in toluene (40 ml) and **1** were added in excess. The mixture was stirred at r.t., and the reaction progress was monitored by TLC. After 4 h, the mixture was washed with H_2O to remove the diselenide anion. The org. phase was evaporated to dryness in vacuum, and the residue was dissolved in $CHCl_3$ and chromatographed (silica-gel column; $CHCl_3$/hexane 1:1). The desired product **4a** showed a moderately higher R_f value than **3a**. Yield: 49 mg (50%). UV/VIS (CH_2Cl_2): 647 (3.70), 591 (3.71), 551 (3.92), 516 (4.17), 485 (3.65), 420 (5.43). ^{1}H-NMR ($CDCl_3$, 270 MHz): 8.74–8.95 (*m*, 16 H, pyrrole); 7.25–8.22 (*m*, 38 arom. H); 4.34 (*t*, 2 CH_2O), 3.42 (*t*, 2 CH_2Se); −2.78 (*s*, 4 NH). HR-MS (MALDI-TOF): 1475.3735 (calc. 1475.3639). Fluorescence: λ_{ex} 422, λ_{em} 654. Anal. calc. for $C_{92}H_{66}N_8O_2Se_2$: C 74.99, H 4.51, N 7.60; found: C 74.80, H 4.42, N 7.48.

Synthesis of the Dimer **4b** *from* **3b**. As described for **4a**, with **3b** (100 mg, 0.13 mmol), excessive amounts of TEBA (0.01 g) in toluene (40 ml), and **1**. The desired product **4b** showed a moderately higher R_f value than **3b**. Yield: 44 mg (45%). UV/VIS (CH_2Cl_2): 649 (3.87), 592 (3.91), 553 (4.04), 517 (4.21), 480 (3.97), 420 (5.35). ^{1}H-NMR ($CDCl_3$, 270 MHz): 8.78–8.88 (*m*, 16 H, pyrrole), 7.20–8.22 (*m*, 38 arom. H); 4.22 (*t*, 2 CH_2O); 3.35 (*t*, 2 CH_2Se); 2.40 (*m*, 2 $OCH_2CH_2CH_2Se$); −2.80 (*s*, 4 NH). HR-MS (MALDI-TOF): 1503.4072 (calc. 1503.3952). Fluorescence: λ_{ex} 422, λ_{em} 653 nm. Anal. calc. for $C_{94}H_{70}N_8O_2Se_2$: C 75.19, H 4.70, N 7.46; found: C 75.24, H 4.59, N 7.38.

Synthesis of the Dimer **4c** *from* **3c**. As described for **4a**, with **3c** (100 mg, 0.13 mmol), TEBA (0.01 g) in toluene (40 ml), and **1** was added in excess. The desired product **4c** showed a moderately higher R_f value than **3c**. Yield: 41 mg (42%). UV/VIS (CH_2Cl_2): 651 (3.98), 594 (4.03), 553 (4.12), 519 (4.21), 420 (5.11). ^{1}H-NMR ($CDCl_3$, 270 MHz): 8.74–8.78 (*m*, 16 H, pyrrole); 7.12–8.11 (*m*, 38 arom. H); 4.09 (*t*, 2 CH_2O); 3.27 (*t*, 2 CH_2Se); 2.31 (*m*, 2 $OCH_2CH_2CH_2CH_2Se$); 2.23 (*m*, 2 $OCH_2CH_2CH_2CH_2Se$); −2.77 (*s*, 4 NH). HR-MS (MALDI-TOF): 1531.4449 (1531.4265). Fluorescence: λ_{ex} 422 nm, λ_{em} 654. Anal. calc. for $C_{96}H_{74}N_8O_2Se_2$: C 75.38, H 4.88, N 7.33; found: C 75.42, H 4.77, N 7.29.

Redox-Potential Characterization. The preparation of water-soluble MWCNTs was carried out according to a procedure described in [19]. Briefly, MWCNTs were mixed with Congo Red (CR) using a certain weight ratio (*e.g.*, MWCNTs/CR 5:1) in an agate mortar and ground for 4 h with the addition of little H_2O to avoid agglomeration of the dry CR powder to produce a greenish black mixture of MWCNTs and CR. The MWCNTs/CR mixture was dissolved in H_2O, filtered through a polytetrafluoroethylene (PTFE) filter disc (0.22-μm pore size), and then washed with H_2O to remove the free CR until the filtrate became colorless. The black product obtained was denoted as MWCNTs-CR_{water}, which was immediately dissolved and stored in H_2O after the washing to avoid the rebundling and the loss of the exfoliated nanotubes when dried. Gold electrode (2.0 mm in diameter, from *CHI*, USA) was polished on a slush of alumina (Al_2O_3, 0.05 μm), and then washed in H_2O, HNO_3/EtOH 1:1 under sonication, each for 3 min. Then, 1 μl of 1.0 mg/ml water-soluble MWCNTs were cast onto the clean Au surface and air-dried. To measure the redox potentials of the diselenide-linked porphyrin dimers **4**, a few drops of a 1 mM sample soln. (in DMF) was added onto the water-soluble MWCNTs-modified gold electrode surface and air-dried. The resulting Se-loaded electrode was immersed directly in 0.1M phosphate buffer (pH 7.4), and cyclic voltammetric measurement was then performed at a scan rate of 100 mV/s.

UV/VIS Absorption, Fluorescence and Induced CD Spectral Studies of the Diselenide-Linked Porphyrin Dimer–DNA Interactions. Spectrophotometric titrations of porphyrins **4** with HS DNA were performed in an aq. buffered soln. at 30°. The porphyrin **4** stock solns. were initially prepared in DMF but were diluted with H_2O in preparing the sample solns. The concentration of the HS DNA stock soln. (in base pairs) was determined spectrophotometrically based on the extinction coefficient of 1.31×10^4 M^{-1} cm^{-1} at 260 nm. Different amounts of HS DNA were mixed with the porphyrin **4**, whose final concentration was fixed at 10 μM, in 10 ml of buffer soln. (0.05M *Tris*·HCl, 0.1M NaCl, pH 7.4, with <5% DMF) to prepare a series of porphyrin–HS DNA sample solns. of different molar ratios ($r = c_{DNA}/c_{porphyrin}$) for spectrophotometric measurements in the range of 320–500 nm. Spectrofluorometric titrations (λ_{ex} 422, λ_{em} 630–700 nm) of porphyrins **4** and HS DNA were conducted in a similar manner. Induced CD spectra of **4a**–**4c** with HS DNA were recorded according to a standard procedure. The ratio $c_{DNA}/c_{porphyrin}$ was ranged from 0 to 20.0, and concentrations of porphyrins **4** were fixed at 5 μM.

Measurement of Singlet-Oxygen Production. A W lamp (power rating 50 W) equipped with an optical filter ($\lambda > 500$ nm) was used as the photoirradiation source. The concentrations of DPBF and the porphyrins used were 5×10^{-5} and 1×10^{-6} M, resp. The consumption of DPBF was monitored by its absorbance at its λ_{max} 415 nm as function of photoirradiation time of the porphyrin-DPBF mixture.

REFERENCES

[1] F. C. Meotti, E. C. Stangherlin, G. Zeni, C. W. Nogueira, J. B. T. Rocha, *Environ. Res.* **2004**, *94*, 276.
[2] A. M. M. Mareque, J. M. Faez, L. K. Chistiaens, S. Kohnen, C. Deby, M. Hoebeke, M. Lamy, G. Deby-Dupont, *Redox Rep.* **2004**, *9*, 81.
[3] L. Savegnago, L. G. Pinto, C. R. Jesse, D. Alves, J. B. T. Rocha, C. W. Nogueira, G. Zeni, *Eur. J. Pharmacol.* **2007**, *555*, 129.
[4] B. S. Reddy, T. T. Wynn, K. El-Bayoumy, P. Upadhyaya, E. Fiala, C. V. Rao, *Anticancer Res.* **1996**, *16*, 1123.
[5] R. M. Rosa, J. D. N. Picada, J. Saffi, J. A. P. Henriques, *Mutat. Res.* **2007**, *628*, 87.
[6] A. F. de Bem, R. D. L. Portella, M. Farina, J. Perottoni, M. W. Paixao, C. W. Nogueira, J. B. T. Rocha, *Basic Clin. Pharmacol. Toxicol.* **2007**, *101*, 47.
[7] L. Letavayova, V. Vlckova, J. Brozmanova, *Toxicology* **2006**, *227*, 1.
[8] M. P. Rayman, *Proc. Nutr. Soc.* **2005**, *64*, 527.
[9] M. E. Reid, M. S. Stratton, A. J. Lillico, M. Fakih, R. Natarajan, L. C. Clark, J. R. Marshall, *J. Trace Elem. Med. Biol.* **2004**, *18*, 69.
[10] J. Y. Zhang, X. J. Wu, X. P. Cao, F. Yang, J. F. Wang, X. Zhou, X. L. Zhang, *Bioorg. Med. Chem. Lett.* **2003**, *13*, 1097.
[11] A. X. Hou, Z. Xue, Y. Liu, S. S. Qu, W. K. Wong, *Chem. Biodiversity* **2007**, *4*, 2889.
[12] J. C. Stockert, M. Canete, A. Juarranz, A. Villanueva, R. W. Horobin, J. I. Borrell, J. Texido, S. Nonell, *Curr. Med. Chem.* **2007**, *14*, 997.
[13] X. Chen, H. Li, D. A. Foster, M. C. Drain, *Biochemistry* **2004**, *43*, 10918.
[14] C. Lottner, K.-C. Bart, G. Bernhardt, H. Brunner *J. Med. Chem.* **2002**, *45*, 2064.
[15] J. V. Vadgama, Y. Wu, D. Shen, S. Hsia, J. Block, *Anticancer Res.* **2000**, *20*, 1391.
[16] H. P. Li, *Bioorg. Med. Chem. Lett.* **2006**, *16*, 6298.
[17] D. L Klayman, T. S. Griffin, *J. Am. Chem. Soc.* **1973**, *95*, 197.
[18] H. S. He, Z. X. Zhao, W. K. Wong, K. F. Li, J. X. Meng, K. W. Cheah, *Dalton Trans.* **2003**, *5*, 980.
[19] C. G. Hu, C. H. Yang, S. S. Hu, *Electrochem. Commun.* **2007**, *9*, 128.
[20] B. Nygaard, *Ark. Kemi* **1967**, *27*, 325.
[21] Y. Ishikawa, N. Yamakawa, T. Uno, *Bioorg. Med. Chem.* **2007**, *15*, 5230.
[22] P. Lugo-Ponce, D. R. McMillin, *Coord. Chem. Rev.* **2000**, *208*, 169.
[23] S. Mettath, B. R. Munson, R. K. Pandey, *Bioconjugate Chem.* **1999**, *10*, 94.
[24] K. Wang, S. T. Fu, L. Wu, Z. Y. Li, *Mendeleev Commun.* **2007**, *17*, 37.
[25] M. A. Sari, J. P. Battioni, D. Duprt, D. Mansuy, J. B. Le Pecq, *Biochemistry* **1990**, *29*, 4205.
[26] R. F. Pasternack, M. Caccam, B. Keogh, T. A. Stephenson, A. P. Williams, E. J. Gibbs, *J. Am. Chem. Soc.* **1991**, *113*, 6835.
[27] S. Yellappa, J. Seetharamappa, L. M. Rogers, R. Chitta, R. P. Singhal, F. D'Souza, *Bioconjugate Chem.* **2006**, *17*, 1418; R. F. Pasternack, *Chirality* **2003**, *15*, 329.
[28] W. Freyer, S. Mueller, K. Teuchner, *J. Photochem. Photobiol.* **2004**, *163*, 231.

Received May 8, 2008